Current Science International
Volume: 15 | Issue: 03| July – Sept.| 2026

EISSN:2706-7920 ISSN: 2077-4435
DOI: 10.36632/csi/2026.15.3.16
Journal homepage: www.curresweb.com
Pages: 192-216

Heavy Minerals Comparison Study from Beach Sand Deposits in Southwest Mauritania and Northern Delta, Egypt

A. El Azab and S.M. El Alfi

Nuclear Materials Authority. P.O. Box 530, El Maadi, Cairo, Egypt.

Received: 10 June 2026 **Accepted:** 20 July 2026 **Published:** 15 August 2026

ABSTRACT

Mauritania is located at the west of Africa, it is border with western desert, and Algeria from north, Mali from east, Senegal from south, and the Atlantic Ocean from west. The total length of the coast is of 667 km. The studies concerned the heavy minerals from Mauritania and comparison by heavy minerals in Egypt. The geomorphologic units are similar and the heavy minerals content nearly similar but in Egypt is progress and build Baltim- El Burullus factory. The volume of sediments in Egypt is bigger than the volume of sediments in Mauritania where the River Nile transport the sediments form the south Africa and path in nine countries but the sediments of Mauritania transported by the branch from the Senegal River and the almost of sediments deposited in Senegal country. The total length of the coast in Egypt is longer and widest. The effect of Mediterranean Sea on the sediments by sorting is more active than Atlantic Ocean. The total heavy minerals in Mauritania represented in Beach by 6.78%, coastal plain by 5.90%, Sand Dunes by 5.96%, and Sabkha by 5.16%, while the total economic minerals represented in Beach by 2.272%, coastal plain by 1.675%, Sand Dunes by 2.082%, and Sabkha by 1.631%. The difference between the total heavy minerals and total economic minerals considers green silicates (gangue minerals).

Keywords: Heavy minerals, Mauritania, northern delta, geomorpholov, Coastal Sand Dunes, Sabkha

1. Introduction

Mauritania is located at the west of Africa, it is border with western desert, Algeria, Mali and Senegal. The west is determined by the Atlantic Ocean. The total length of the coast is of 667 km (Fig. 1a).

The current geological exploration work has been accomplished in support of the wide exploration program, included in a project of mineral sand assessment along the Atlantic Ocean Coast of Mauritania. The delineated area (Fig. 1b) lies about 120km south Nouakchott city and extended for about 20km length to south ward, while its average width about 6km, it is bounded by the beach from the west, and the high way (N2) to the east ward. You can reach the Port of Nouakchott city at a distance of 120km by the high way who brings Rosso city to Nouakchott city (N2) (Fig.1a).

The climate of Mauritania is dry and high temperature in July, August and September. September is hotter, the temperature is about 24 ~ 34°C. December is colder, the temperature is about 13 ~ 28°C, each year, of September to December there are a lot of wind and of sand, the corrosion of salt is violent. The amount of rain annual average is of only 53 mm.

The mineral resources in Mauritania located in the sand beach of the Atlantic Ocean, which restricted in the west of the country. The industry has not developed in the region, minerals exploration mining is restricted to iron ore, gold and the copper.

This project is a new project, the unit of building is Mauritania Titanium Resources S.A., it is dedicated to the development and to the use of resources mineral in the territory of Mauritania. The

Corresponding Author: S.M. El Alfi, Nuclear Materials Authority. P.O. Box 530, El Maadi, Cairo, Egypt.
E-mail: samehelalfi2@gmail.com

resources black sands are developed in cooperation with the Mauritania, the Government of Mauritania holds a share of 20% of the company MTR.

Proving of such data required detailed fieldwork, which includes geologic and geomorphological exploration studies.

Geomorphologic Units

The coastal environment is the area lying at the interface between the land and the sea. The coastal environment includes both the zone of shallow water within which waves are able to move sediment, and the area land-ward of this zone, including beaches, coastal plains, coastal dunes, and sabkha areas. These landforms are affected to some degree by the direct or indirect effects of marine waves, tides and currents.

Therefore, the morphological descriptions of the southern part of Mauritania sand dunes can be adopted to the description of Breed and Grow (1979). The southern part of Mauritania is geomorphologically formed of a wide plain gradually sloping westward to the Atlantic Ocean. It occupies about 120 km^2 and a great part of its surface is mainly covered by wind-borne sands accumulated as sand dune. The dunes are generally extending almost parallel to the regional structure of the area. The coastal zone of this area is characterized by various types of sand dunes forming large belts extending along the Atlantic Ocean shoreline.

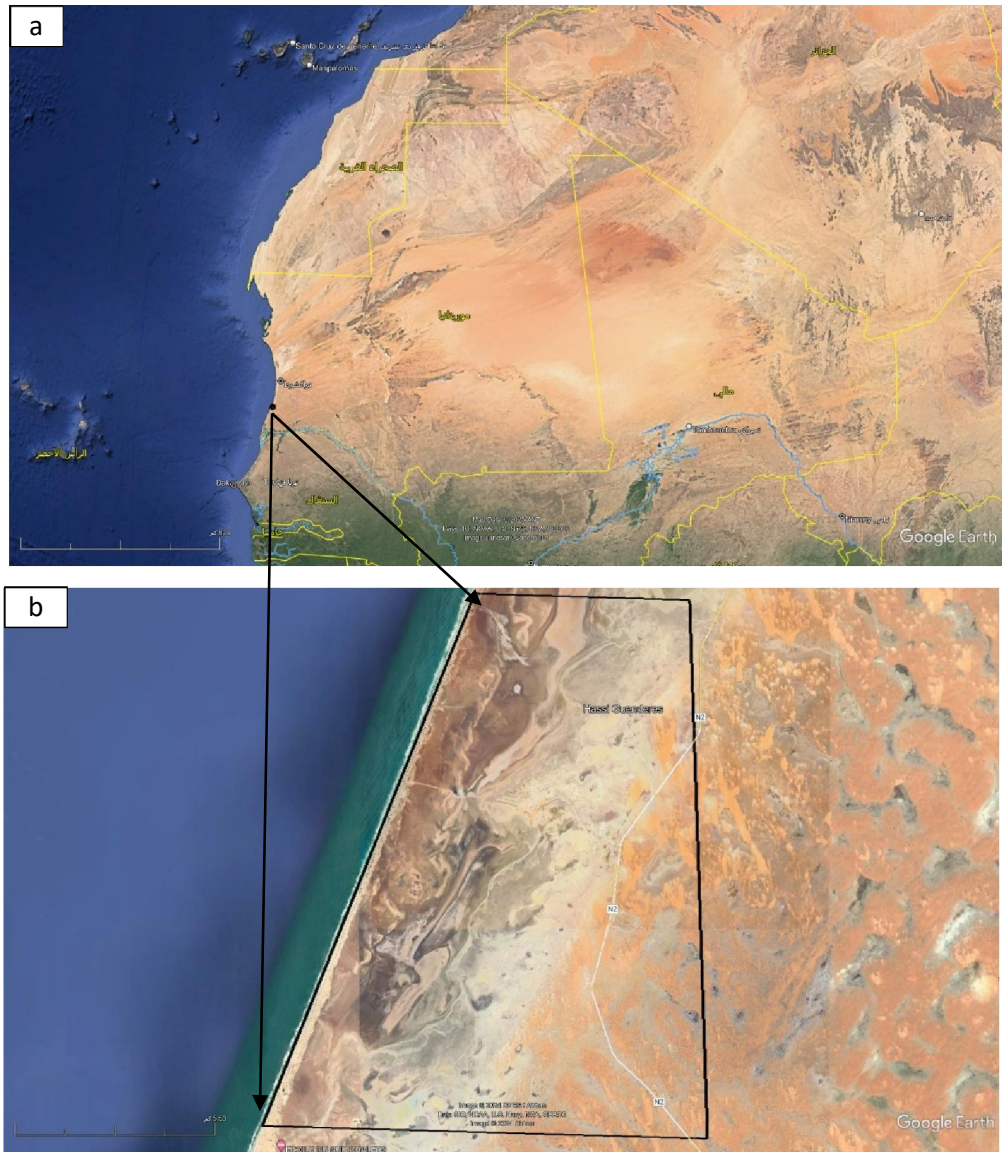


Fig. 1: a) Mauritania location map from Google earth, b) the studied area location map

1. Beach (Shoreline)

The configuration of the shape of Mauritania coast is the result of wave, tides, currents erosions and deposition. Waves and tides involve the movement and dissipation of large amount of energy and this is capable to causing rapid and spectacular changes in landforms along the coastlines (Summerfield, 1991). The length of coastal environment of the study area extends for about 20 kilometers, and form sandy coast.

The prevailing long shore current, in Atlantic from South to North, constantly modifies the shores and reshape coastlines with less activity of waves and currents. The Mauritania beaches are composed of unconsolidated and readily transportable sand, occasionally, they can adjust quickly to changes in the nature and energy of coastal processes. The Holocene has been great changes in the position of shorelines and in coastal morphology as a result of predominantly rising sea levels (Summerfield, 1991).

Shoreline processes can change in intensity from day to day, and from season to season but they never stop. According to Keller, (2000), winds generated waves period yield most of the energy for shoreline processes. One of the most important shoreline processes is the long-shore drift current which generates by waves attack (rework) obliquely lowland the shore.

Erosion along a coast tends to occur until equilibrium is established between wave energy and the configuration of the shore. Sediment transported by waves and long shore current is deposited in area of low energy to form beaches, spits and barrier islands. Erosion and deposition along the Mauritania coasts tend to develop straight and gently curved shorelines. These shapes are in equilibrium with the energy expended upon it.

The shoreline (or coastline) separates the coast from the ocean and represented the geographical area affected by wave action. The shape of the coastlines is mainly concave or, convex or, straight and formed from main line segments have NE, and minor segments of E-W to WNW trends. The shoreline is a narrow stretch with gentle slope toward the ocean where the beach in that area represents accretion zone. The beach (shoreline) is primarily made up of quartz sand (very fine to coarse) with amounts of shell fragments, and heavy minerals (Fig. 2a, b &c). Large asymmetric cusps reach height 50 cm are recognized along the beach in the study area (Fig. 2a &b). The average width of the shore is about 5-10m (Fig. 2c), ended by berm rising about half meter (50cm.) above sea level.

2. Coastal Plain

The coastal area, is the land and ocean areas bordering the shore line. While the coastal plain is an area of lowland adjacent to the ocean, and resulting from the accumulation of marine or alluvial sediments. Where formed by marine sediments the coastal plain has been exposed by a relative fall of pea-level. However, the coastal line is that line forms the boundary between the coast and the shore, commonly forms boundary between land and water.

The area is flat, and elevated few centimeters to meters than the sea, so it submerged by water in winter season where the ocean level is rising. The coastal plain is wide, its width is ranging between 50 to 200m (Fig. 3a &b). It is flat and covered by black sand deposits, where the sea affected on it by transgression and regression. This plain has been used as extending for a beach, building for fisher and farmers, or mining of heavy minerals from black sand (Fig. 3c &d)). Also, some parts of this area were used building of village for fisher and farmers.

3. Coastal Sand Dunes

Various types of sand dunes can be identified according to their external shape, special arrangement and orientation. Two types of sand dunes are observed in the study area; namely (in order of abundance): linear (longitudinal) dunes (Fig. 4a &b), and barchan dunes (Fig. 4c &d). The different types of sand dunes in the area can summarize in table 1.

Coastal dunes of longitudinal and barchan types are composed of fine, and medium-grain-sized quartz sand. However, they may also comprise of shell fragments, and heavy minerals.

a) Linear dunes are the most abundant aeolian landform in the coast area. They are extending along the coastal zone of the Atlantic Ocean. They are mostly ancient fixed dunes of different types with smooth vegetated surfaces. It consists of an array of parallel to sub-parallel vegetated linear dunes. Along the study area, the most pronounced feature of these linear dunes is the occurrence of their flanks facing the north and south directions. In some localities the northern flanks are steeper than the southern ones.

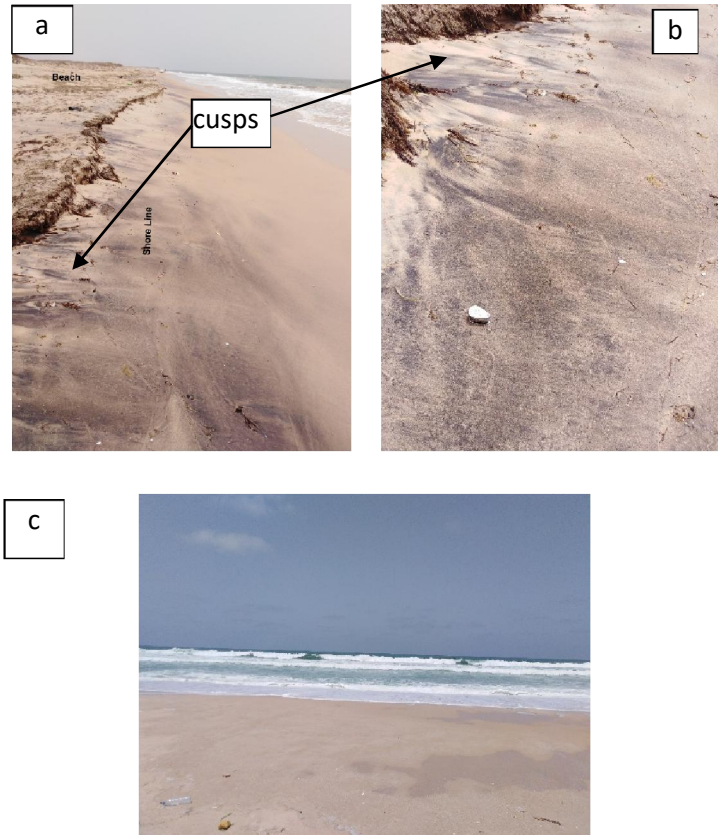


Fig. 2: Photomicrographs Shows: The beach with Black sand and the cusps.

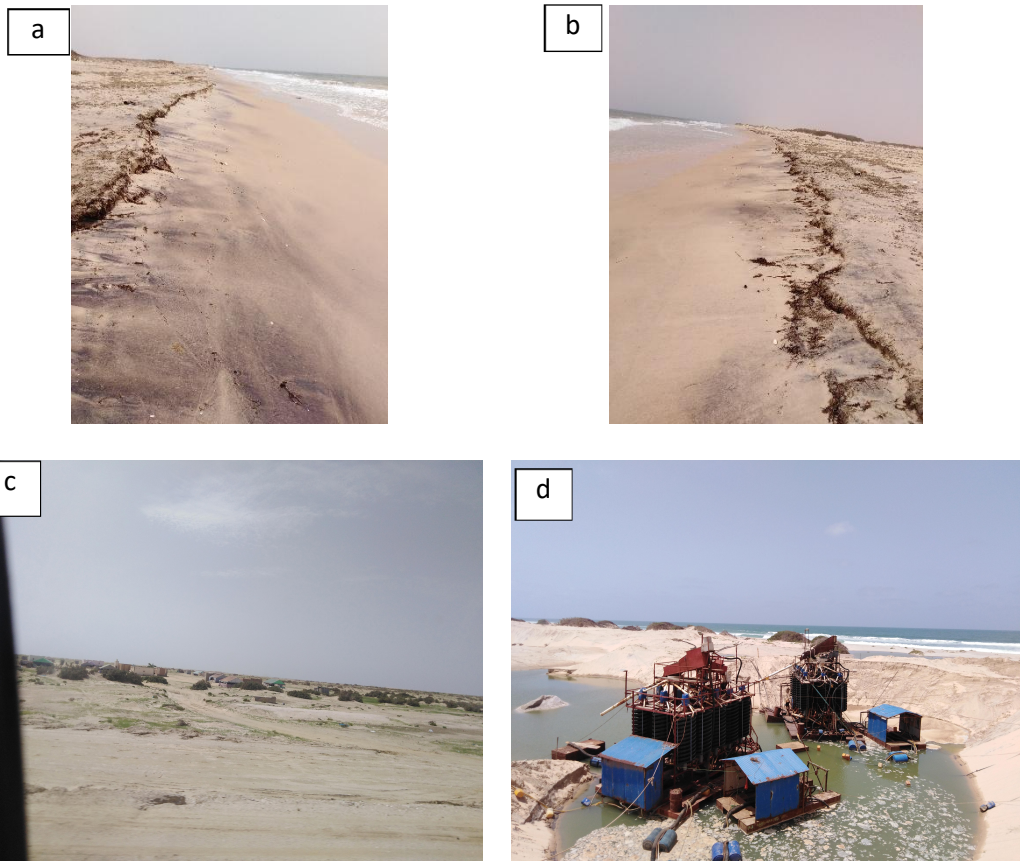


Fig. 3: Photomicrographs Shows: a, b) The coastal plain width ranging from 50-200m, c) The Building of fishers and farmers, d) The Mining Equipment (Spirals)

b) The barchan dunes are pronounced, particularly along the beach (Fig. 4c &d). These dunes are slightly high (up to 15m), devoid of vegetation and migrate toward the NE direction.

The inter-dune depressions vary in shape, depending on the morphometric of the individual dune, as well as the distribution pattern of the neighboring dunes. They are generally flat-topped and very densely vegetated.

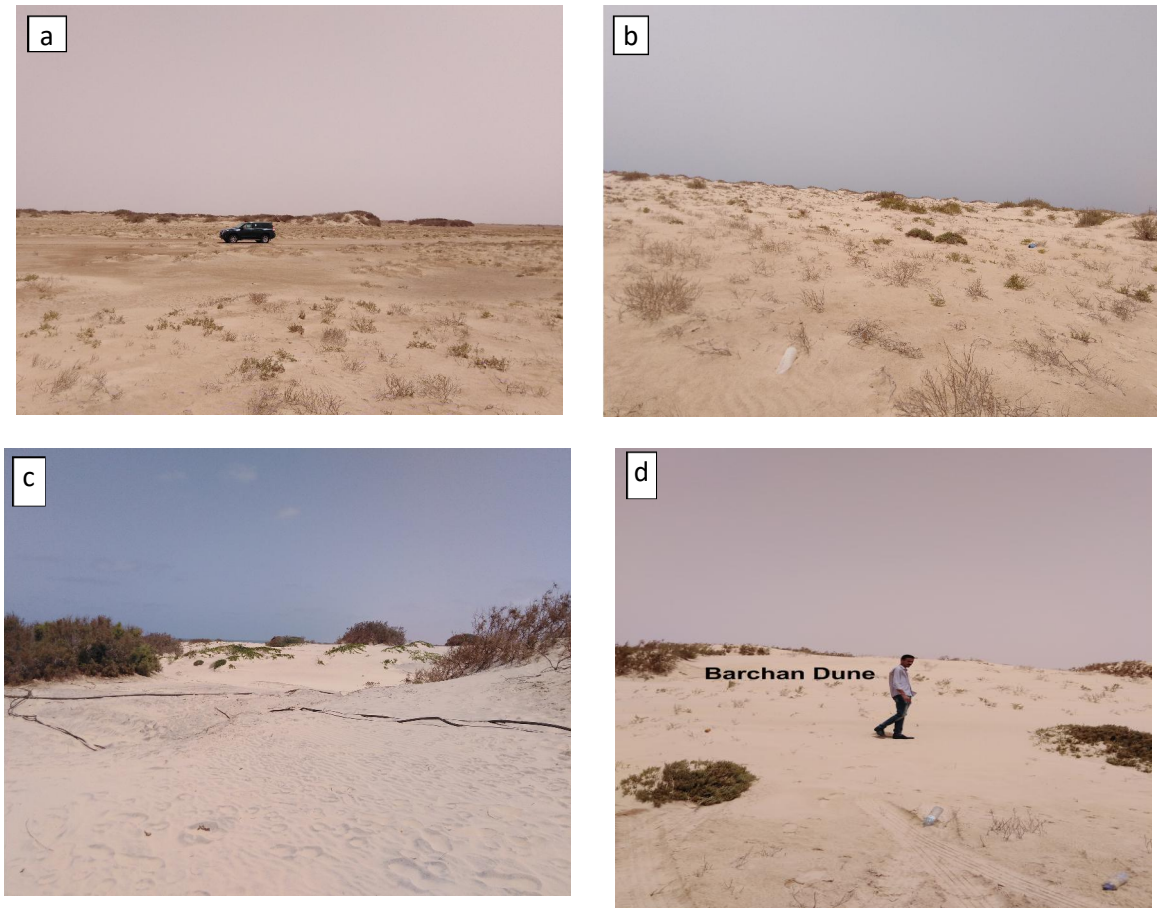


Fig. 4: photomicrographs Shows: a &b) Linear (Longitudinal) dune, c) Barchan Dune and d) Barchan Dune

Table 1: The morphometric parameters of barchans, and linear dunes of the area.

Type	Direction	Height (m)	Length (m)	Width (m)
Linear	N-S	about 15	150-250	20
Barchan	NE-SW	10-15	10-100	15-20

4. Sabkha

Sabkha is a flat low land, mostly located near the coastal shore. Sabkha in the study area are scattered around the area (Fig. 5a &b). Also, sabkhas were formed in the intertidal-supratidal zone, where the land is low and composed of fine-grained clastic sediments. In the Trucial sabkha gypsum and anhydrite are the dominant evaporite minerals (Kinsman, 1969).



Fig. 5: Photomicrographs Shows: a) Sabkha as flat area and bounded by linear dune and b) Sabkha area

2. Materials and Methods

Sampling

A program for systematic drilling was executed in the dune belt in order to obtain representative sampling from the different parts of the belt. The drilling program was designed considering the geomorphologic condition. The manual auger-like drilling methods were used in the drilling and collected representative samples. These drilling methods were successfully applied before in many countries as Egypt (El Burullus dune belt as reported in NMA v.2, 2003), that was verified and approved by Mineral Technology (MT) Australia and Snowden Australian consultant for minerals.

Field Sampling Distribution

The study area divided into different divisions according to the geomorphic units covered by boreholes on grid pattern (Fig. 6). The distance between each borehole ranging from 500m to 1000m based on what accessibility and covered the area. The distribution of the boreholes is covering the project area. Bore hole spacing is relatively wider and such distribution of the boreholes represents a reconnaissance study. The area covered by 60 samples represented by 15 samples in beach area (Fig. 7a), 15 samples in coastal area (Fig. 7b), 15 samples in sand dune area (Fig. 7c), and 15 samples in sabkha area (Fig. 7d).

Preparation of Samples and Techniques

All mineral species with a specific gravity of more than 2.88g/cm^3 are traditionally considered as heavy minerals. Mohamed (1998) stated that the total heavy minerals were concentrated in the medium, fine and very fine sand size fractions so These investigations were done on the sand size less than 0.5mm. The study area is covered by 60 samples. The original sand sample was dried, and prepared for mineral separation using bromoform (Sp. Gr. 2.88 g/cm^3). Heavy fractions were dried, weighted and their percentages were calculated and tabulated in table (2). The light fractions were discarded, while the heavy fraction is used for further analysis.

The magnetite separation carried out using a small hand magnet with suitable strength. The magnetite free heavy minerals assemblage was magnetically fractionated using the laboratory Frantz Isodynamic Magnetic Separator (Model L-1) at side slope of 5°, forward slope of 20° (Flinter,1955). Mineralogical investigation of the mineral constituents was carried out by Semi-quantitative EDX and the chemical analyses were carried out using a Phillips and Griffen (1981) XL-30 Environmental Scanning Electron Microscope (ESEM) on individual grains of heavy minerals.

3. Results and Discussion

The most important heavy minerals will be described in the following paragraphs:

The separated heavy minerals were then studied under a Binocular Stereomicroscope and were classified into two main groups according to Folk (1980). The first is the opaque as; magnetite, ilmenite, leucoxene and pyrite and the second is the non-opaque include zircon, garnet, monazite, rutile, titanite, gahnite and green silicates (pyroxene and amphibole groups, epidote and mica group). The percentage

of each mineral is calculated to the original samples and averages of the total heavy mineral for the studied sediments are tabulated in Tables (3a, b, c &d).

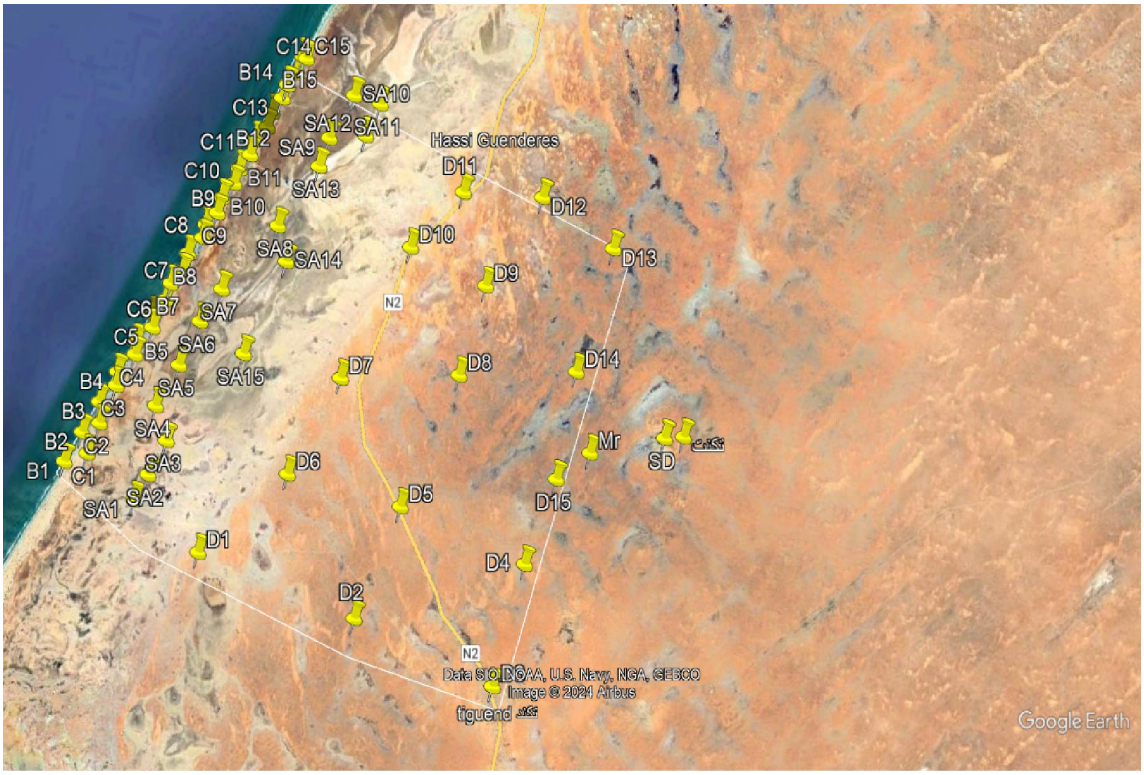


Fig.6: Shows the samples distribution in different Geomorphic Units

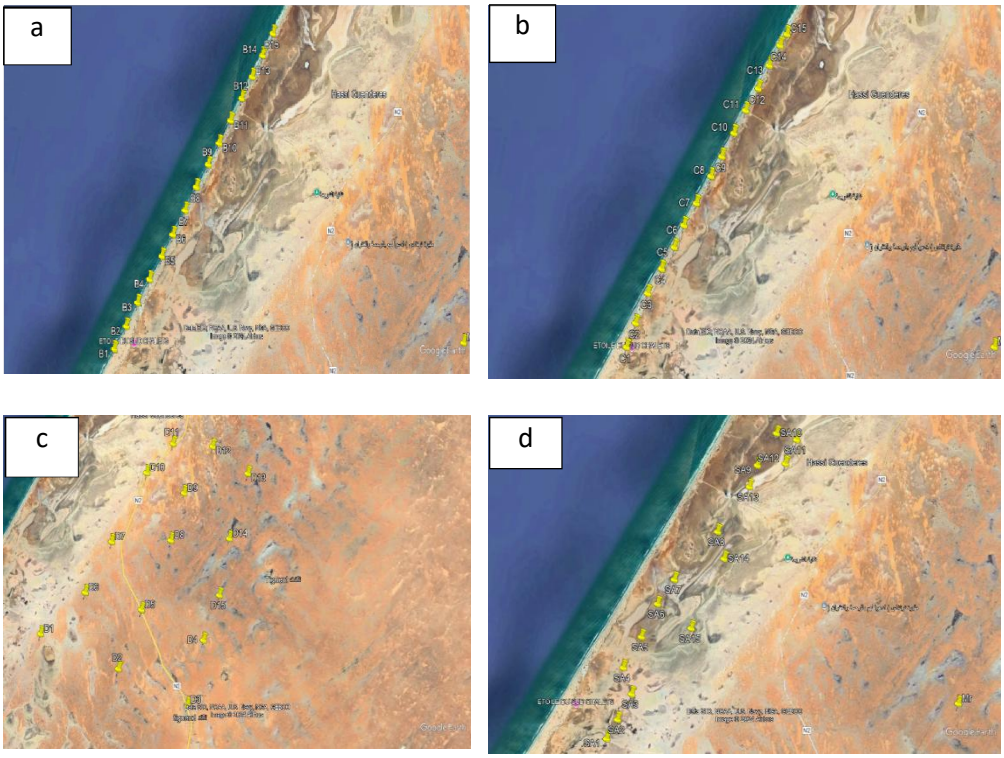


Fig. 7: Shows: a) The samples location in Beach Geomorphic unites, b) The samples location in Coastal Geomorphic unites, c) The samples location in Sand Dunes Geomorphic unites and d) The samples location in Sabkha Geomorphic unites.

Table 2: Percentages of total heavy minerals after bromoform for the studied sediments.

Beach environment		Coastal environment		Dune environment		Sabkha environment	
S. No.	**H.Br. %**	**S. No.**	**H.Br. %**	**S. No.**	**H.Br. %**	**S. No.**	**H.Br. %**
B1	4.1	C16	4.0	D31	7.8	SA46	5.4
B2	3.9	C17	4.3	D32	8.2	SA47	3.8
B3	5.1	C18	6.1	D33	6.5	SA48	5.1
B4	5.6	C19	5.2	D34	6.9	SA49	5.3
B5	6.3	C20	6.1	D35	9.6	SA50	6.6
B6	4.2	C21	8.04	D36	6.5	SA51	5.0
B7	8.2	C22	4.2	D37	5.0	SA52	6.4
B8	8.7	C23	5.6	D38	5.8	SA53	7.4
B9	6.5	C24	8.1	D39	4.7	SA54	4.16
B10	7.2	C25	6.5	D40	4.8	SA55	2.06
B11	10.1	C26	5.6	D41	4.1	SA56	4.2
B12	9.8	C27	8.76	D42	6.75	SA57	4.3
B13	6.7	C28	5.8	D43	4.0	SA58	5.6
B14	6.8	C29	4.1	D44	4.2	SA59	4.9
B15	8.46	C30	6.11	D45	4.6	SA60	7.2
Min.	3.90	Min.	4.00	Min.	4.00	Min.	2.06
Max.	10.10	Max.	8.76	Max.	9.60	Max.	7.40
Ave.	6.78	Ave.	5.90	Ave.	5.96	Ave.	5.16

S. No. Sample Number, H. Br. = Heavy Bromoform

Table 3a: The percentage of total heavy minerals for beach samples

S. N.	Mg.%	Ilm. %	Gar. %	Rut. %	Lux.%	Zr. %	Mz. %	T. Ec.%	G. S.%	T. H. %
B1	0.04	1	0.02	0.03	0.09	0.03	0.01	1.22	2.88	4.1
B2	0.03	0.82	0.11	0.01	0.25	0.02	0.01	1.25	2.65	3.9
B3	0.04	1.25	0.04	0.01	0.22	0.03	0.01	1.6	3.5	5.1
B4	0.04	1.25	0.04	0.05	0.3	0.03	0.01	1.72	3.88	5.6
B5	0.4	1.28	0.05	0.01	0.22	0.01	0.01	1.98	4.32	6.3
B6	0.04	0.92	0.04	0.04	0.09	0.03	0.01	1.17	3.03	4.2
B7	0.2	1.57	0.05	0.04	0.59	0.11	0.01	2.57	5.63	8.2
B8	0.1	1.89	0.15	0.02	0.42	0.01	0.001	2.59	6.11	8.7
B9	0.4	1.03	0.2	0.04	0.4	0.05	0.02	2.14	4.36	6.5
B10	0.4	1.2	0.35	0.04	0.68	0.12	0.05	2.84	4.36	7.2
B11	1.3	1.79	0.2	0.11	0.78	0.4	0.03	4.61	5.49	10.1
B12	1	1.83	0.15	0.05	0.57	0.19	0.01	3.8	6	9.8
B13	0.7	1.06	0.04	0.01	0.11	0.02	0.01	1.95	4.75	6.7
B14	0.14	1	0.05	0.03	0.78	0.09	0.01	2.1	4.7	6.8
B15	0.2	1.53	0.19	0.04	0.47	0.1	0.01	2.54	5.92	8.46
Min.	0.030	0.820	0.020	0.010	0.090	0.010	0.001	1.170	2.650	3.900
Max.	1.300	1.890	0.350	0.110	0.780	0.400	0.050	4.610	6.110	10.100
Ave.	0.335	1.295	0.112	0.035	0.398	0.083	0.014	2.272	4.505	6.777

S. No.=Sample number, Mg.=magnetite, Ilm. =Ilmenite, Gar. =Garnet, Lux. =Leucoxene, Rut. =Rutile, Zr. =Zircon, Mz. =Monazite, G.S.=Green silicates, T. Ec. = Total Economic Minerals, T. H., = Total Heavy Minerals

Table 3b: The percentage of total heavy minerals for Coastal Plain Samples

S. NO.	Mg.%	Ilm. %	Gar. %	Rut. %	Lux.%	Zr. %	Mz. %	T. Ec. %	G. S. %	T. H. %
C16	0.32	0.65	0.01	0.02	0.02	0.003	0.004	1.027	2.973	4
C17	0.35	0.58	0.01	0.03	0.06	0.01	0.001	1.041	3.259	4.3
C18	0.8	0.9	0.05	0.02	0.04	0.01	0.005	1.825	4.275	6.1
C19	0.6	0.78	0.02	0.04	0.06	0.02	0.01	1.53	3.67	5.2
C20	0.7	1.1	0.03	0.01	0.12	0.01	0.01	1.98	4.12	6.1
C21	0.16	1.02	0.06	0.05	0.15	0.01	0.002	1.452	6.59	8.042
C22	0.1	0.5	0.08	0.03	0.11	0.2	0.01	1.03	3.17	4.2
C23	0.4	1.1	0.04	0.01	0.09	0.01	0.03	1.68	3.92	5.6
C24	0.93	1.2	0.04	0.02	0.33	0.07	0.01	2.6	5.5	8.1
C25	0.5	1.1	0.07	0.02	0.32	0.06	0.002	2.07	4.43	6.5
C26	0.14	1.26	0.06	0.04	0.22	0.07	0.01	1.8	3.8	5.6
C27	1	1.1	0.05	0.02	0.1	0.05	0.01	2.33	6.43	8.76
C28	0.8	0.8	0.04	0.1	0.12	0.03	0.01	1.9	3.9	5.8
C29	0.2	0.61	0.01	0.15	0.02	0.01	0.004	1.004	3.096	4.1
C30	0.4	1.03	0.05	0.03	0.13	0.2	0.02	1.86	4.25	6.11
Min.	0.100	0.500	0.010	0.010	0.020	0.003	0.001	1.004	2.973	4.000
Max.	1.000	1.260	0.080	0.150	0.330	0.200	0.030	2.600	6.590	8.760
Ave.	0.493	0.915	0.041	0.039	0.126	0.051	0.009	1.675	4.226	5.901

S. No. = Sample Number, Mg. = Magnetite, Ilm. = Ilmenite, Gar. = Garnet, Lux.= Leucoxene, Rut. = Rutile, Zr. = Zircon, Mz. = Monazite, G.S.= Green silicates, T. Ec. = Total Economic Minerals, T. H., = Total Heavy Minerals

Table 3c: The percentage of total heavy minerals for sand Dunes Samples

S. N.	Mg.%	Ilm. %	Gar. %	Rut. %	Lux.%	Zr. %	Mz. %	T. Ec. %	G. S.%	T. H. %
D31	0.2	1.5	0.05	0.04	0.59	0.11	0.01	2.5	5.3	7.8
D32	0.1	1.8	0.15	0.02	0.42	0.01	0.001	2.5	5.7	8.2
D33	0.4	1.03	0.2	0.04	0.4	0.05	0.02	2.14	4.36	6.5
D34	0.4	0.95	0.3	0.06	0.3	0.12	0.05	2.18	4.72	6.9
D35	0.8	0.9	0.2	0.11	0.7	0.4	0.03	3.14	6.46	9.6
D36	0.52	0.7	0.15	0.05	0.5	0.19	0.01	2.12	4.38	6.5
D37	0.7	1.06	0.04	0.01	0.11	0.02	0.01	1.95	3.05	5
D38	0.14	1	0.05	0.03	0.78	0.09	0.01	2.1	3.7	5.8
D39	0.2	1.53	0.19	0.04	0.47	0.1	0.01	2.54	2.16	4.7
D40	0.4	0.75	0.07	0.02	0.11	0.15	0.01	1.51	3.29	4.8
D41	0.1	1.1	0.12	0.01	0.24	0.08	0.01	1.66	2.44	4.1
D42	0.14	1.5	0.08	0.05	0.36	0.02	0.004	2.15	4.6	6.75
D43	0.1	1.07	0.02	0.08	0.03	0.02	0.003	1.32	2.68	4
D44	0.5	1	0.01	0.01	0.1	0.01	0.01	1.64	2.56	4.2
D45	0.1	1.44	0.07	0.02	0.13	0.01	0.01	1.78	2.82	4.6
Min.	0.100	0.700	0.010	0.010	0.030	0.010	0.001	1.320	2.160	4.000
Max.	0.800	1.800	0.300	0.110	0.780	0.400	0.050	3.140	6.460	9.600
Ave.	0.320	1.155	0.113	0.039	0.349	0.092	0.013	2.082	3.881	5.963

S. No. = Sample Number, Mg. = Magnetite, Ilm. = Ilmenite, Gar. = Garnet, Lux. = Leucoxene, Rut. = Rutile, Zr. = Zircon, Mz. = Monazite, G.S. = Green silicates, T. Ec. = Total Economic Minerals, T. H., = Total Heavy Minerals

Table 3d: The percentage of total heavy minerals for Sabkha Samples

S. No.	Mg.%	Ilm. %	Gar. %	Rut. %	Lux.%	Zr. %	Mz. %	T. C.%	G.S.%	T. H %
SA46	0.05	1.1	0.16	0.04	0.3	0.02	0.03	1.7	3.7	5.4
SA47	0.4	0.5	0.05	0.05	0.22	0.01	0.01	1.24	2.56	3.8
SA48	0.3	0.8	0.04	0.02	0.33	0.07	0.01	1.57	3.53	5.1
SA49	0.7	0.4	0.03	0.1	0.2	0.01	0.01	1.45	3.85	5.3
SA50	0.2	1.4	0.06	0.04	0.72	0.13	0.02	2.57	4.03	6.6
SA51	0.4	0.4	0.02	0.06	0.37	0.01	0.01	1.27	3.73	5
SA52	0.4	1.1	0.16	0.01	0.19	0.16	0.03	2.05	4.35	6.4
SA53	0.1	1.2	0.4	0.03	0.75	0.03	0.05	2.56	4.84	7.4
SA54	0.14	0.4	0.2	0.1	0.42	0.07	0.01	1.34	2.82	4.16
SA55	0.1	0.3	0.01	0.02	0.16	0.06	0.01	0.66	1.4	2.06
SA56	0.3	0.5	0.1	0.05	0.13	0.2	0.02	1.3	2.9	4.2
SA57	0.2	0.4	0.1	0.1	0.3	0.07	0.01	1.18	3.12	4.3
SA58	0.2	0.8	0.2	0.04	0.24	0.22	0.03	1.73	3.87	5.6
SA59	0.03	0.52	0.23	0.03	0.4	0.28	0.04	1.53	3.37	4.9
SA60	0.5	1.34	0.07	0.02	0.32	0.06	0.01	2.32	4.88	7.2
Min.	0.030	0.300	0.010	0.010	0.130	0.010	0.010	0.660	1.400	2.060
Max.	0.700	1.400	0.400	0.100	0.750	0.280	0.050	2.570	4.880	7.400
Ave.	0.268	0.744	0.122	0.047	0.337	0.093	0.020	1.631	3.530	5.161

S. No. = Sample Number, Mg. = Magnetite, Ilm. = Ilmenite, Gar. = Garnet, Lux. = Leucoxene, Rut. = Rutile, Zr. = Zircon, Mz. = Monazite, G.S. = Green silicates, T. Ec. = Total Economic Minerals, T. H., = Total Heavy Minerals

Opaque minerals

Magnetite (Fe^{2+}, Fe_2^{3+} O_4)

Magnetite displays black to deep reddish-brown color, with metallic to dull luster. The brownish tint can be attributed to their alteration and/or oxidation process, in addition to the probable presence of exsolved ilmenite and /or hematite. These minerals occur either separately from each other or in homogenous fixed compounds or as inclusions within each other (Mücke 2003). Different types of magnetite –ilmenite intergrowths and their origin were studied previously by many workers (Boctor 1966; Basta 1972; Arafa 1990; Dewedar 1998; El Balakssy 2003; Hassaan 2005; Mansour 2009; Barakat 2016). Due to the preferred incorporation of the elements Mg, Mn, Zn, Ni, Cr, Ti, Al, V in the magnetite lattice, naturally occurring magnetite always has varying percentages of these elements

Magnetite habit ranges from massive, granular, angular, sub-angular to sub-rounded (Fig. 8a) and the octahedron crystals of magnetite are less frequent and occur as isolated grains. Magnetite has abnormal shapes like spherical (Fig. 8b) and drops (Fig. 8c). These abnormal shapes are formed when the grains moved downward in air when they were in molten state. Some of these grains are massive (Fig. 8d) whereas most of them contains air gaps of different sizes or entirely emptied (Fig. 8e &f). the periphery of the abnormal shapes from inside shows different thickness (Fig. 8e) whereas the outside was shown in figure (8f). some of magnetite grains shows different degrees of alteration (Fig. 8g) and others attached with other minerals on its surface like azurite (Fig.8c) and malachite (Fig. 8h)

Picked magnetite grains investigated using ESEM is shown in figure (9) which shows Spherical grains (Fig. 9a), drop grains with air gaps of different sizes (Fig. 9b), drop grains (Fig. 9c), the outside view of the abnormal spherical shape (Fig. 9d) and altered magnetite grains (Fig. 9e).

The average of semi-quantitative chemical analysis of magnetite in the studied area were tabulated in table (4) which compared with other analysis in different locations in Egypt in the same table.

Magnetite was recorded in all studied sediments and its content range from 0.03% to 1.30% with an average of 0.335% in beach, range from 0.1% to 1.0% with an average of 0.493% in coastal plain, range from 0.1% to 0.8% with an average of 0.32% in sand dune and range from 0.03% to 0.7% with an average of 0.268% in sabkha.

Ilmenite $FeTiO_3$

Ilmenite is considered as the most important ore of titanium, consequently, it is used as a raw material for pigment production, paints, printing inks, plastics, rubber, artificial fibers, paper, glass and ceramics (Elsner, 2010). Ilmenite is a ferromagnetic mineral separated mainly at the magnetic fields 0.2A and 0.5A. The significance of ilmenite as the most important rock-forming titanium mineral is not due to titanium extraction but for the production of titanium dioxide (TiO_2), so it is economically important and considered as a major source of titanium and a minor source of iron (Zhang *et al.,* 2011). Titanium dioxide is easily the most significant white pigment in the world.

Ilmenite was recorded as iron-black with metallic luster. It occurs as aggregates with different shapes (Fig. 10a), triangular shape (Fig. 10b), oval shape (Fig. 10c), rounded to subrounded and discoidal shapes (Fig. 10d) and micasious shape (Fig. 10e). It is more abundant in the fine sand size than that of the medium sand size fractions.

Picked ilmenite grains were investigated under using ESEM and their chemical composition are shown in figure (11) which shows Irregular shapes (Fig. 11a &b), triangular shape (Fig. 11c), angular to sub-angular with sharp edges (Fig. 11d), rounded to sub-rounded (Fig. 11e) and f) oval shape (Fig. 11f).

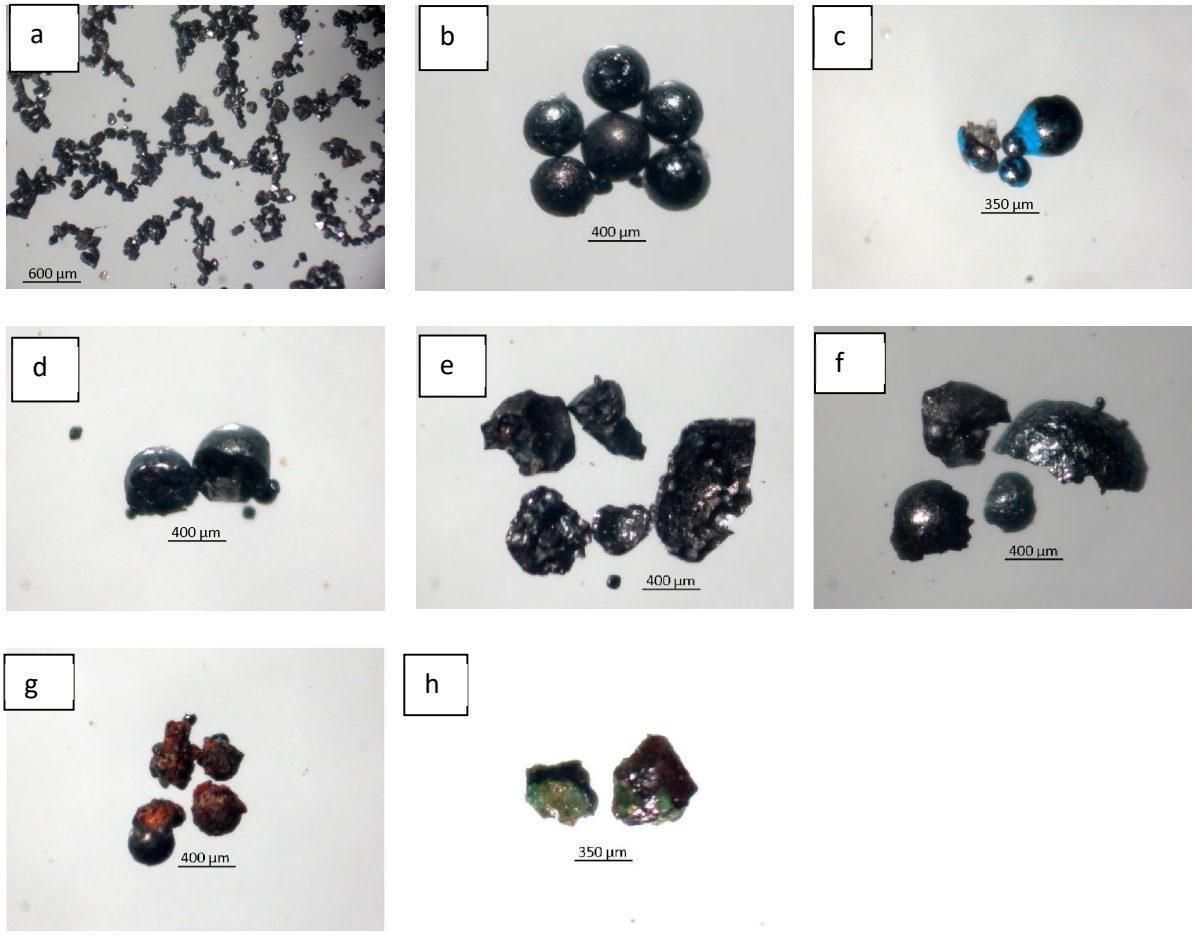


Fig. 8: Photomicrographs of magnetite grains show: a) Aggregates of sub-angular and sub-rounded grains, spherical grains, b) Spherical grains, c) Drop grains with azurite mineral attached on its surface, d) Massive spherical grains, e) The inside view of the abnormal spherical shape showing different thickness, f) The outside view of the abnormal spherical shape, g) Altered magnetite grains, h) sub-angular grains with malachite mineral attached on its surface.

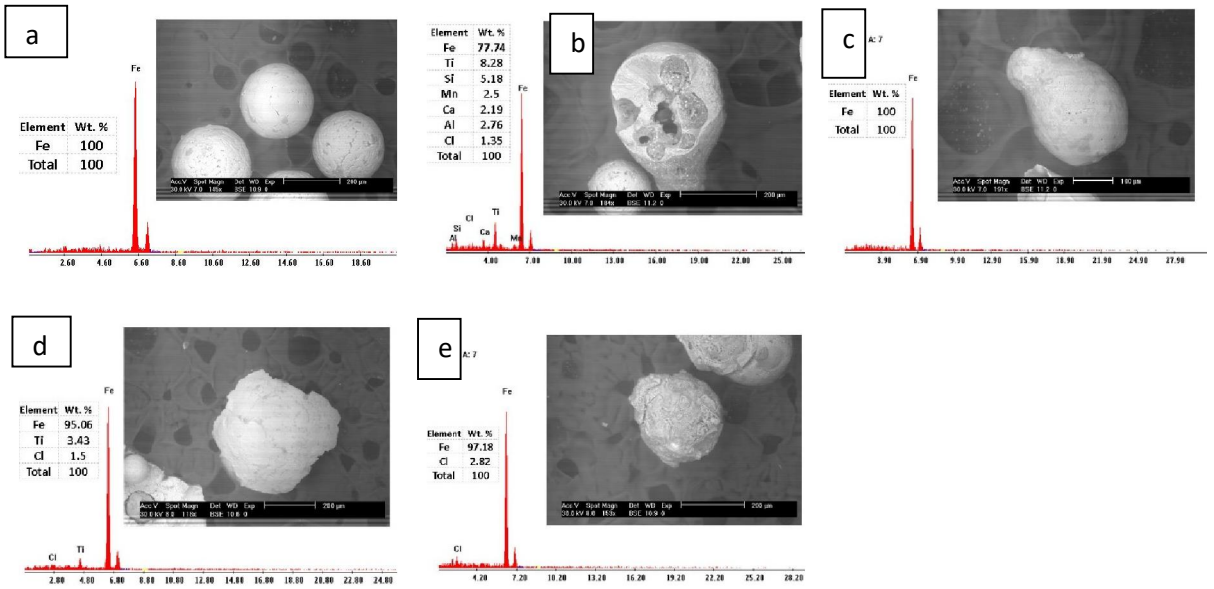


Fig. 9: EDX and BSE image of magnetite grain shows: a) Spherical grains, b) Drop grains with air gaps of different sizes, c) Drop grains, d) The outside view of the abnormal spherical shape and e) Altered magnetite grains.

Table 4: The average semi quantitative chemical analysis of magnetite in the studied area compared with different localities in Egypt.

Element Wt. %	Mauritania (present study)	Barakat (2016) East Rashied		El Azab *et al.* (2019) Damietta	El Alfi (2019) West El-Burullus	Awad *et al.* (2022) El Arish	El Afandy (2022) North delta
		Normal grains	Rounded and oval grains				
Fe	93.18	85.042	90.29	70.34	75.24	84.73	77.57
Ti	5.86	6.201	1.27	26.71	16.83	14.78	16.83
Si	4.52	3.252	0.47	2.18	2.37	10.38	2.37
Mn	2.50	0.623	0.51		3.49		3.49
Ca	2.84	0.493	0.79	0.76		1.53	
Al	2.76	2.085	2.17		2.07	4.35	2.07
Cl	2.24						
S	2.54						

The average of semi-quantitative chemical analysis of ilmenite in the studied area were tabulated in table (5) which compared with other analysis in different locations in Egypt in the same table.

Ilmenite was recorded in all studied sediments and its content range from 0.82% to 1.89% with an average of 1.295% in beach, range from 0.5% to 1.26% with an average of 0.915% in coastal plain, range from 0.70% to 1.8% with an average of 1.155% in sand dune and range from 0.3% to 1.4% with an average of 0.744% in sabkha.

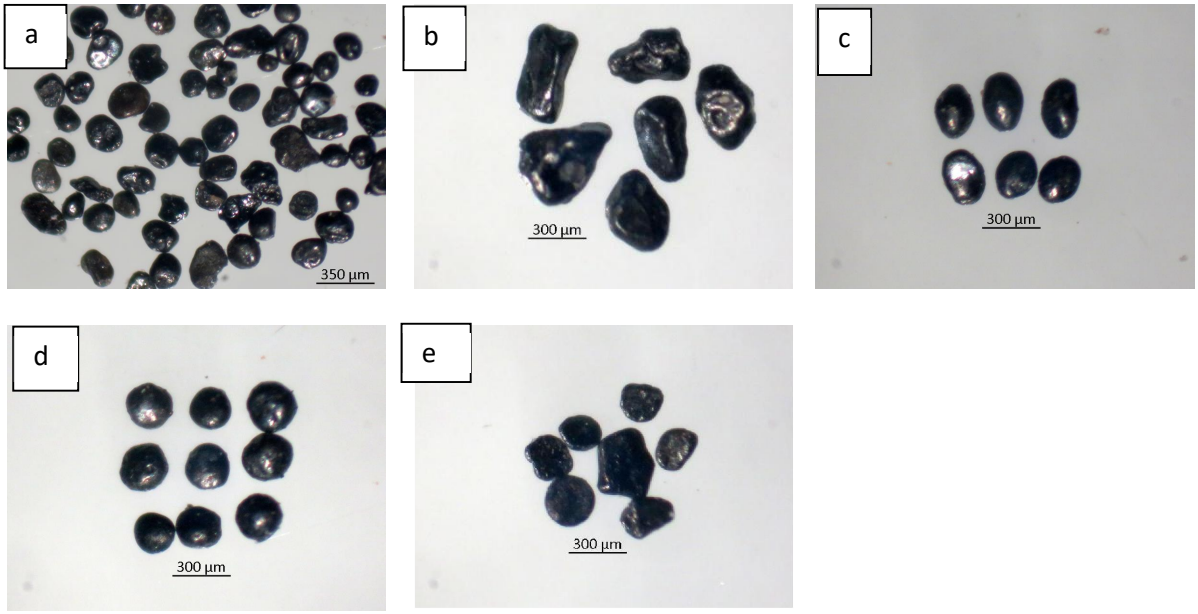


Fig. 10: Photomicrograph of ilmenite grains shows: a) Different aggregates with different shapes, b) triangular shape, c) Oval shape, d), Rounded to subrounded and discoidal shapes and e) Micasious shape.

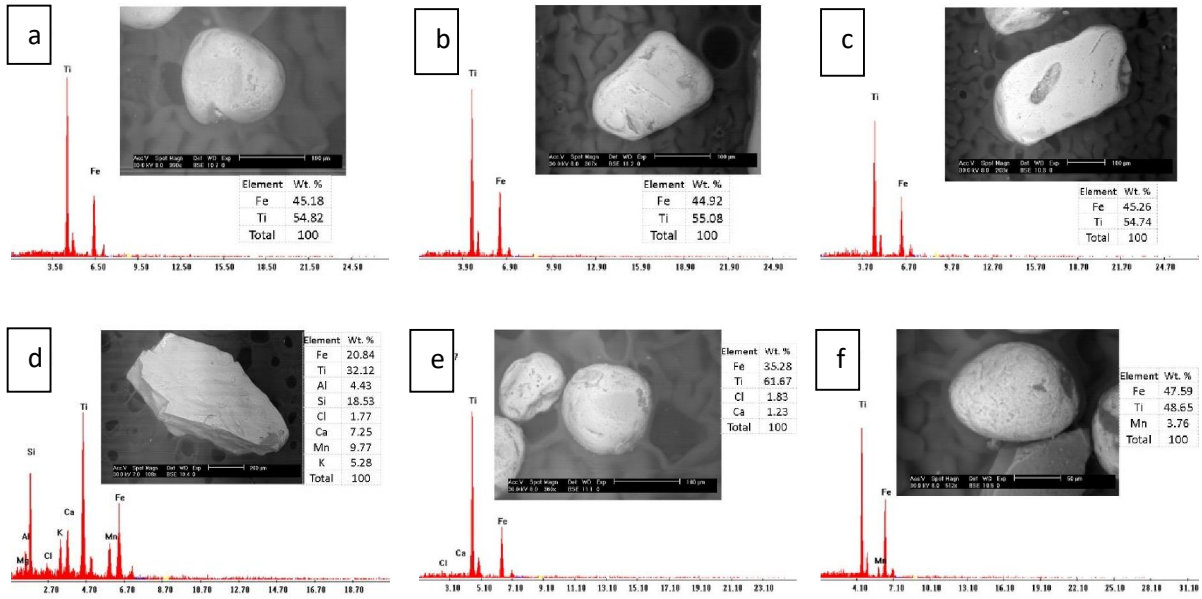


Figure (11): EDX and BSE image of ilmenite grains shows: a &b) Irregular shapes, c) Triangular shape, d) Angular to sub-angular with sharp edges, e) Rounded to sub-rounded and f) Oval shape

Table 5: The average semi quantitative chemical analysis of ilmenite in the studied area compared with different localities in Egypt.

Element Wt. %	Mauritania (present study)	Barakat (2016) East Rashied	El Azab *et al.* (2019) Damietta	El Alfi (2019) West El-Burullus	Awad *et al.* (2022) El Arish	El Afandy (2022) North delta
Fe	42.07	45.77	41.70	33.98	35.23	45.64
Ti	49.00	49.17	46.49	59.34	58.62	50.35
Al	3.99	0.60		1.95	2.88	
Si	10.54	1.16	1.215	2.94	4.95	
Cl	2.95					
Ca	3.31	0.50			1.39	
Mn	5.06	0.71		1.8	4.11	4.01
K	5.28	0.19				

Leucoxene ($FeTiO_3$)

Leucoxene represents a transitional alteration product of ilmenite to form secondary rutile (Mohamed, 1987;Mohamed, 1998; Elsner, 2010). The inherent color of leucoxene depends on the degree of alteration and TiO_2 content. Leucoxination process does not only affect the overall grade, but also changes the density of mineral grains (Temple, 1966) and their magnetic susceptibility (Frost *et al*., 1986). Both SiO_2 and Al_2O_3 impurity levels in the grains increase with increasing of leucoxination degree (Hugo and Cornell, 1991). The alteration process of ilmenite grains commonly started from outside to inside along exsolution lamellae, twin planes, cracks and other zones of weaknesses. According to the degree of alteration, the leucoxene color changes from black, brown, yellow to white.

Leucoxene was separated at 0.5A and 1.0A but the majority were separated at 1.0A. Its grains range from irregular forms and colors (Fig. 12a), oval, rounded to sub-rounded and discoidal shapes with smooth or pitted surface (Fig. 12b). Ilmenite occurs as relicts on the surface of leucoxene indicating the alteration processes (Fig. 12c).

Picked leucoxene grains were investigated using ESEM and their chemical composition is shown in figure (13) which shows rounded grains (Fig. 13a), discoidal grains (Fig. 13b), oval grains (Fig. 13c) and relicts of ilmenite in leucoxene grains (Fig. 13d).

The average of semi-quantitative chemical analysis of leucoxene in the studied area were tabulated in table (6) which compared with other analysis in different locations in Egypt in the same table

Leucoxene was recorded in all studied sediments and its content range from 0.09% to 0.78% with an average of 0.398% in beach, range from 0.02% to 0.33% with an average of 0.126% in coastal plain, range from 0.03% to 0.78% with an average of 0.349% in sand dune and range from 0.13% to 0.75% with an average of 0.337% in sabkha.

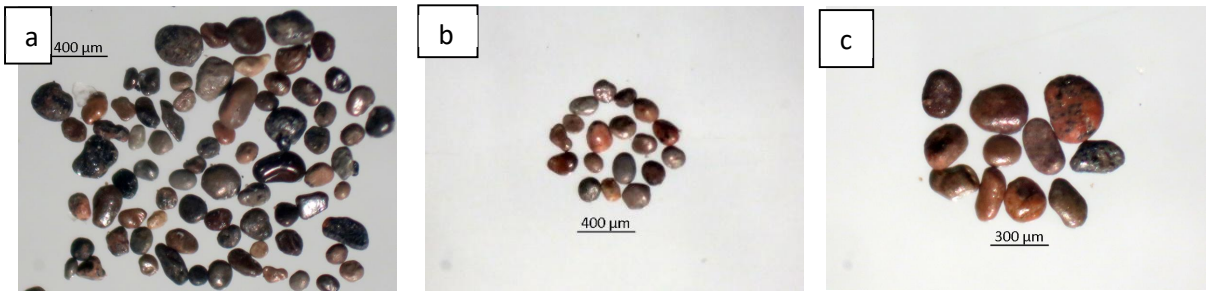


Fig. 12: Photomicrographs of leucoxene grains shows: a) Different forms and colors of leucoxene grains, b) oval, rounded, sub-rounded and discoidal forms and c) Residual ilmenite particles within leucoxene grains.

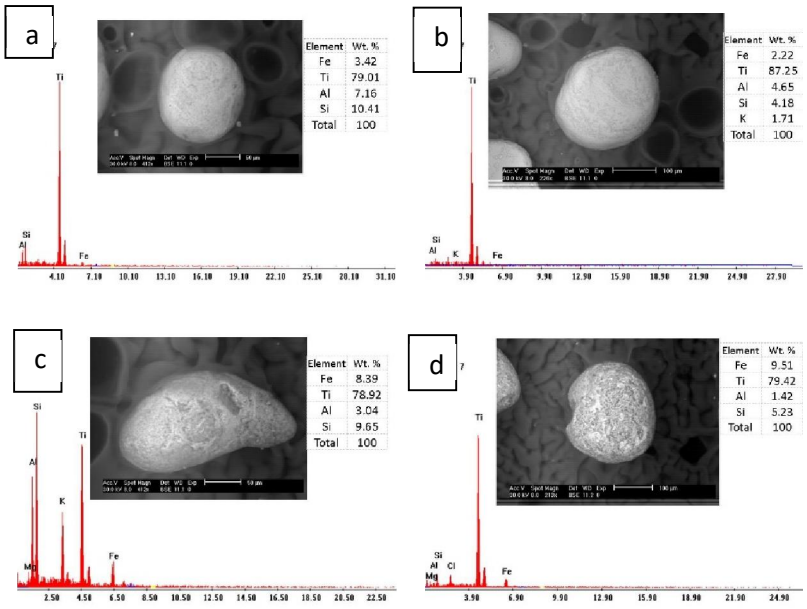


Fig. 13: EDX and BSE image of leucoxene grain shows: a) rounded grains, b) discoidal grains, c) oval grains and d) relicts of ilmenite in leucoxene grains.

Table 6: The average semi quantitative chemical analysis of leucoxene in the studied area compared with different localities in Egypt.

Element Wt. %	Mauritania (present study)	Barakat 2016 East Rashied	El Azab *et al.* (2019) Damietta	El Alfi (2019) West El-Burullus	Awad *et al.* (2022) El Arish
Fe	7.24	14.45	2.29	3.32	10.83
Ti	78.69	76.16	70.03	64.61	87.33
Al	5.07	2.19	0.84	1.21	
Si	8.00	4.68	0.21	3.01	
K	1.29	0.13	1.32		
Cl	4.43				
Cr		0.11	2.29		

NON-OPAQUE MINERALS

Zircon ($ZrSiO_4$)

Most of zircon grains have a euhedral external morphology. It is concentrated in both non-magnetic and magnetic fractions at 1.5A. Zircon separated in the nonmagnetic field 1.5A have long prismatic water clear color with vitreous luster. Armstrong (1922); Groves (1930); Poldervaart (1955-1956) and Saxena (1966) stated that the water clear zircon grains in all types of rocks are nonmagnetic. According to Rozendaal & Philander (2000), zircon can be grouped into four types as follow: - a) Clear zircons contain low levels of Fe, U and Th. b) Pink zircons contain moderate levels of rare earths (REE), U and Th. c) Yellow zircons contain high levels of REE, U, Th, Fe, Al, P and Ca and d) Metamict zircons contain very high levels of REE, U, Th, Fe and Y.

It was recorded as colorless short to long prismatic with or without bipyramidal termination (Fig. 14a), colorless sub-rounded to rounded and oval forms (Fig. 14b), light yellow oval grains (Fig. 14c), white prismatic with smooth curved edges (Fig. 14d), light purple sub-rounded grains (Fig. 14e) and black short prismatic with bipyramidal termination (Fig. 14f)

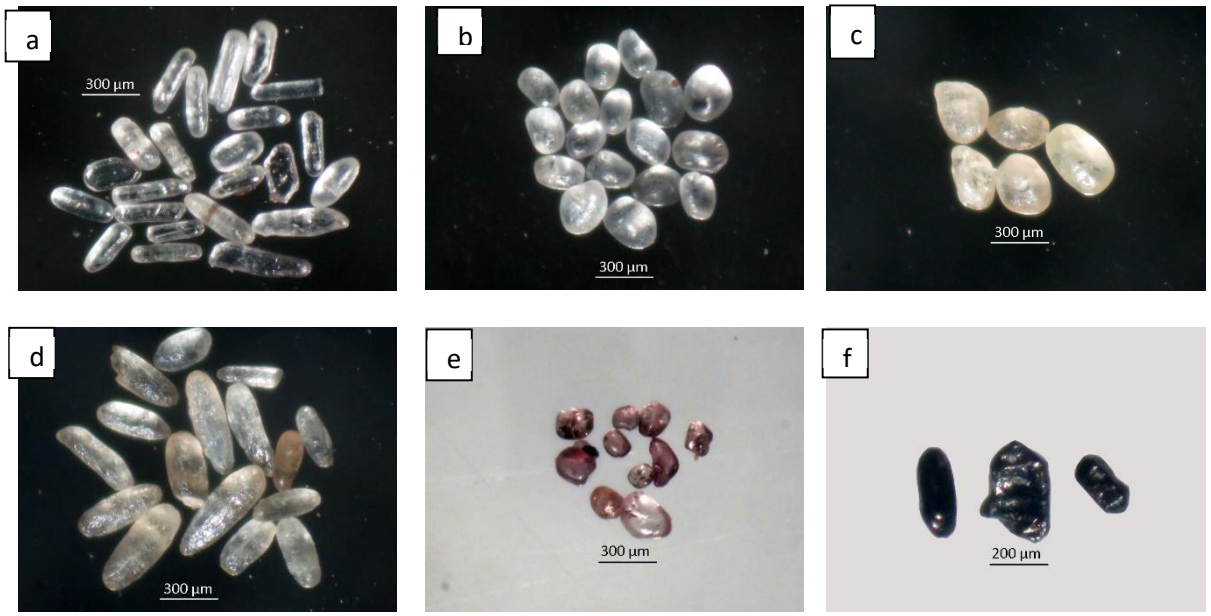


Fig. (14): Photomicrographs of zircon grains shows: a) Colorless short to long prismatic with or without bipyramidal termination, b) Colorless sub-rounded to rounded and oval forms, c) Light yellow oval grains, d) White prismatic with smooth curved edges, e) light purple sub-rounded grains, f) Black short prismatic with bipyramidal termination

Picked zircon grains were investigated using ESEM and their chemical compositions are shown in figure (15) which shows colorless long prismatic grain (Fig. 15a), colorless short prismatic grain (Fig. 15b), sub-rounded grain (Fig. 15c), yellow oval grain (Fig. 15d), colorless long prismatic with smooth curved edge (Fig. 15e) and black short prismatic grain showing outgrowth (Fig. 15f).

The average of semi-quantitative chemical analysis of zircon in the studied area were tabulated in table (7) which compared with other analysis in different locations in Egypt in the same table.

Zircon was recorded in all studied sediments and its content range from 0.01% to 0.4% with an average of 0.083% in beach, range from 0.003% to 0.2% with an average of 0.051% in coastal plain, range from 0.01% to 0.4% with an average of 0.092% in sand dune and range from 0.01% to 0.28% with an average of 0.093% in sabkha.

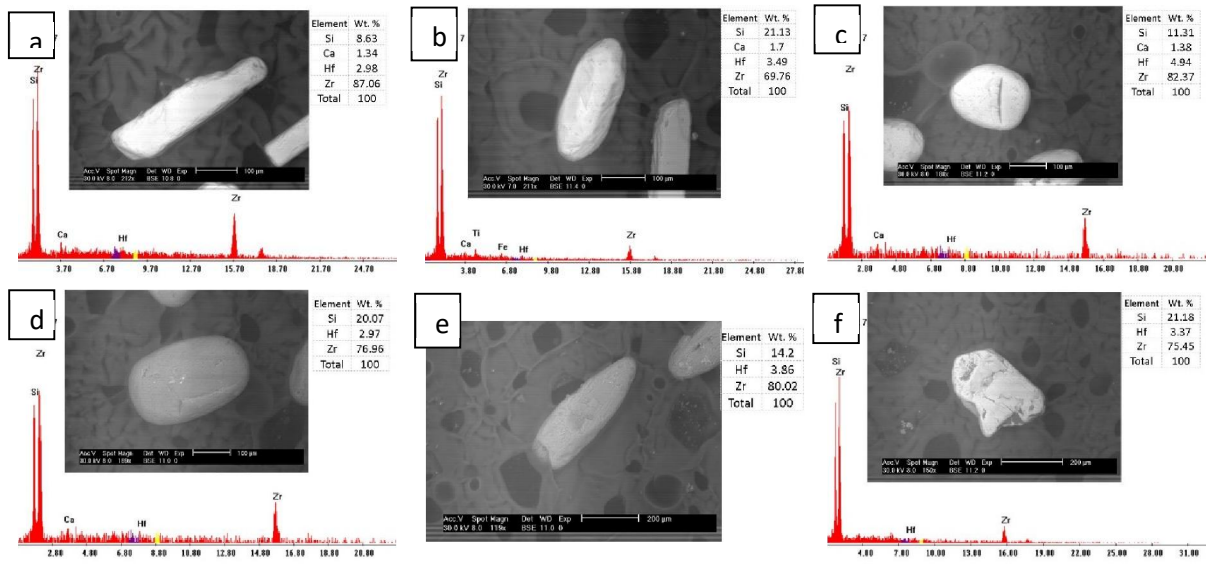


Fig. 15): EDX and BSE images of pure zircon grain shows: a) Colorless long prismatic grain, b) Colorless short prismatic grain, c) sub-rounded grain, d) Yellow oval grain, e) Colorless long prismatic with smooth curved edge and f) black short prismatic grain showing outgrowth.

Table 7: The average semi quantitative chemical analysis of zircon in the studied area compared with different localities in Egypt.

Element Wt. %	Mauritania (present study)	Barakat (2016) East Rashied	El Azab *et al.* (2019) Damietta	El Alfi (2019) West El-Burullus	Awad *et al.* (2022) El Arish	El Afandy 2022 North Delta
Si	17.01	64.47	17.80	16.99	21.07	49.41
Ca	1.47	0.49	0.92	1.49	1.37	
Hf	3.12	3.62	2.83	2.80	4.34	2.71
Zr	78.24	60.85	58.26	74.84	67.05	47.89
Fe		1.51	26.51	2.20	2.06	
U		0.50		2.83	0.74	
Al		0.99			1.33	
Th		0.46			2.04	

Garnet

Garnet is a group of minerals closely have physical and chemical properties. The minerals of garnet group characterize some metamorphic rocks, others occur in high-pressure igneous rocks. Garnet was separated at magnetic field strength 0.2A and 0.5A. it was recorded in the studied samples light rose almandine grains (Fig. 16a), deep rose almandine grains (Fig. 16b), red almandine grains (Fig. 16c) and colorless grossularite grains (Fig. 16d).

Picked garnet grains were investigated using ESEM and their chemical compositions are shown in Figures (17) which shows right rose almandine garnet (Fig. 17a &b), deep rose almandine garnet (Fig. 17c &d), red almandine garnet (Fig. 17e) and colorless grossularite garnet (Fig. 17f).

The average of semi-quantitative chemical analysis of garnet in the studied area were tabulated in table (8) which compared with other analysis in different locations in Egypt in the same table.

Garnet was recorded in all studied sediments and its content range from 0.02% to 0.35% with an average of 0.112% in beach, range from 0.01% to 0.08% with an average of 0.041% in coastal plain, range from 0.01% to 0.3% with an average of 0.113% in sand dune and range from 0.01% to 0.4% with an average of 0.122% in sabkha.

Monazite [$CeLaPO_4$]

It is rare earth phosphate mineral of highly variable composition. In reality, monazite technically four different minerals technically, but because of a lack of great differences between them they are referred to as one mineral monazite. The four monazites have differences in the percentages of their chemical constituents. Their differences are reflected in their respective names (Van Emden *et al*., 1997):

1. (Ce)-Monazite: (Ce, La, Nd, Th, Y)PO_4
2. (La)-Monazite: (La, Ce, Nd)PO_4
3. (Nd)-Monazite: (Nd, La, Ce)PO_4
4. (Sm)-Monazite: (Sm, Gd, Ce, Th)PO_4

Monazite is radioactive due to the presence of thorium and, less commonly, uranium. Because of its radioactive nature, monazite is useful for radiometric dating of geological events, such as crystallization, heating, or deformation of rocks.

Their color ranges from colorless, lemon yellow, light red and deep red to black (Fig. 18a). They occur as accessory mineral in the fine and very fine sand fractions. It was separated at magnetic field strength 0.5A and 1.0A. Monazite exhibits shape varies between rounded, discoidal, oval and prismatic.

Picked monazite grains were investigated using ESEM and their chemical compositions are shown in figure (18) which shows red discoidal grains (Fig. 18b) and black oval grains (Fig. 18c). the monazite in the present study belongs to (Ce)-Monazite: (Ce, La, Nd, Th, Y) PO_4.

The average of semi-quantitative chemical analysis of garnet in the studied area were tabulated in table (9) which compared with other analysis in different locations in Egypt in the same table.

Monazite was recorded in all studied sediments and its content range from 0.001% to 0.05% with an average of 0.014% in beach, range from 0.001% to 0.03% with an average of 0.009% in coastal

plain, range from 0.001% to 0.05% with an average of 0.013% in sand dune and range from 0.01% to 0.05% with an average of 0.02% in sabkha.

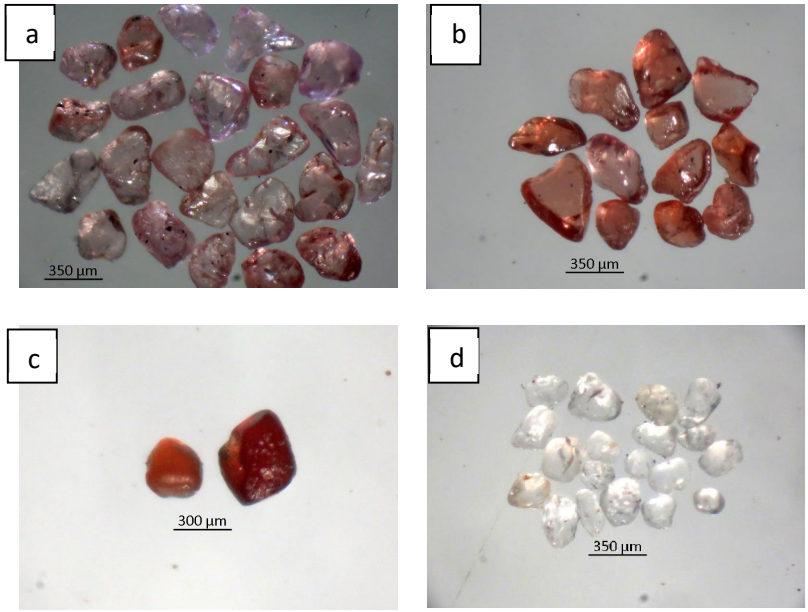


Fig. 16: Photomicrographs of garnet grains show: a) light rose almandine grains, b) Deep rose almandine grains, c) Red almandine grains and e) Colorless grossularite grains.

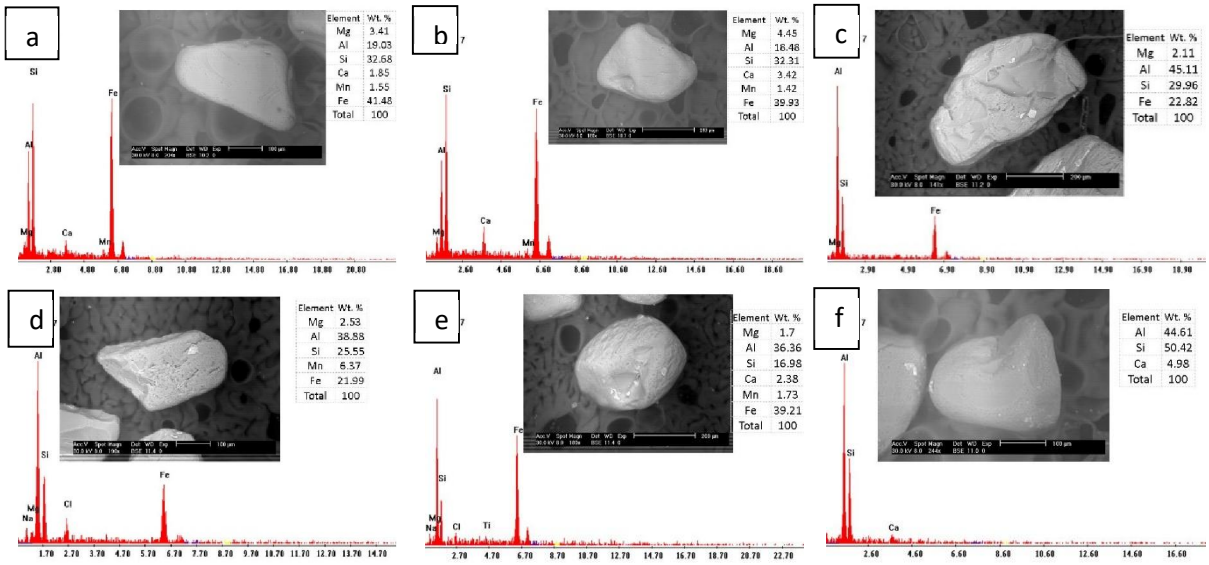


Fig. 17: EDX and BSE image of garnet shows: a &b) Light rose almandine garnet, c &d) Deep rose almandine garnet, e) Red almandine garnet and f) colorless grossularite garnet.

Table 8: The average semi quantitative chemical analysis of garnet in the studied area compared with different localities in Egypt.

Element Wt. %	Mauritania (present study)	Barakat (2016) East Rashied	El Azab *et al.* (2019) Damietta	El Alfi (2019) West El-Burullus	Awad *et al.* (2022) El Arish	El Afandy (2022) North delta
Mg	3.86	6.18	10.17	4.94	3.13	3.86
Al	33.07	21.16	21.48	23.61	19.74	32.09
Si	32.80	35.34	37.79	46.75	34.34	38.21
Ca	6.77	4.61	1.47	4.08	3.49	3.00
Mn	2.31	7.07	--	0.72	7.98	2.48
Fe	26.65	27.68	29.1	19.92	30.56	22.55

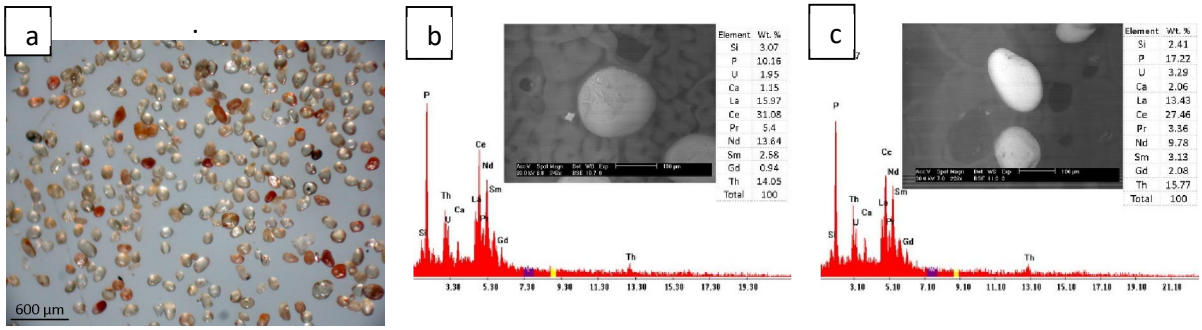


Fig. 18: Photomicrographs of monazite grains shows: a) different shapes and colors grains, b) Red discoidal monazite grains and c) black oval monazite grains.

Table 9: the average semi quantitative chemical analysis of monazite in the studied area compared with different localities in Egypt.

Element Wt. %	Mauritania (present study)	Barakat (2016) East Rashied	El Azab *et al.* (2019) Damietta	El Alfi (2019) West El-Burullus	Awad *et al.* (2022) El Arish	El Afandy (2022) North delta
Si	4.662	0.68	1.51	2.44	3.36	2.11
P	15.214	27.66	19.32	17.64	25.73	22.87
U	2.62	1.16	1.26	2.68	2.19	3.11
Ca	1.252	0.80	1.08	1.00	1.70	1.67
La	14.966	14.23	16.33	17.15	14.09	14.19
Ce	29.86	29.77	33.75	30.62	26.13	28.46
Pr	4.914	--	4.53	4.06	3.81	4.48
Nd	11.718	11.54	12.75	10.91	10.03	11.76
Sm	2.25	2.82	0.71	1.74	2.22	2.28
Gd	1.7825	1.92	--	2.11	1.90	3.59
Th	11.938	6.12	8.73	10.94	11.24	7.30
Fe	3.73	0.20	--	1.01	--	--

Rutile TiO_2

It is considered a major ore of titanium. Rutile occurs as red aggregates of different forms (Fig. 19a), black prismatic grains (Fig. 19b), honey prismatic, chevron and oval grains (Fig. 19c) and oval, semi-rounded and discoidal grains (Fig. 19d).

The main paramagnetic rutile grains were separated at magnetic field strength of 1.5A and the rest diamagnetic rutile were concentrated in the nonmagnetic 1.5A. The opaque variety is frequent in the highly magnetic while yellowish and reddish (translucent) rutile increases in the nonmagnetic fraction. The opaque Fe-Ti minerals such as magnetite, ilmenite and rutile were derived from the volcanic rocks from the Ethiopian plateau (El-Kammar et al., 2010).

Picked rutile grains were investigated using ESEM and their chemical compositions are shown in Figure (20) which shows black prismatic grain (Fig. 20a), red oval grain (Fig. 20b), red irregular grain (Fig. 20c) and black discoidal grain (Fig. 20d).

The average of semi-quantitative chemical analysis of rutile in the studied area were tabulated in table (10) which compared with other analysis in different locations in Egypt in the same table.

Rutile was recorded in all studied sediments and its content range from 0.01% to 0.11% with an average of 0.035% in beach, range from 0.01% to 0.15% with an average of 0.039% in coastal plain, range from 0.01% to 0.11% with an average of 0.039% in sand dune and range from 0.01% to 0.1% with an average of 0.047% in sabkha.

Titanite (Sphene) Ca Ti Si O_5

Titanite is more common in all samples of the studied sediments. Its color varies from Honey grains (Fig. 21a), dark honey to black grains (Fig. 21b) and figure (21c) shows colorless to honey on the left

side and dark honey to black on the right side. Titanite was separated at magnetic field strength 1.0A and less common in 0.5A.

Picked titanite grains were investigated using ESEM and their chemical compositions are showing semi-rounded grain (Fig. 21d) and oval grain (Fig. 21e).

The average of semi-quantitative chemical analysis of rutile in the studied area were tabulated in table (11) which compared with other analysis in different locations in Egypt in the same table.

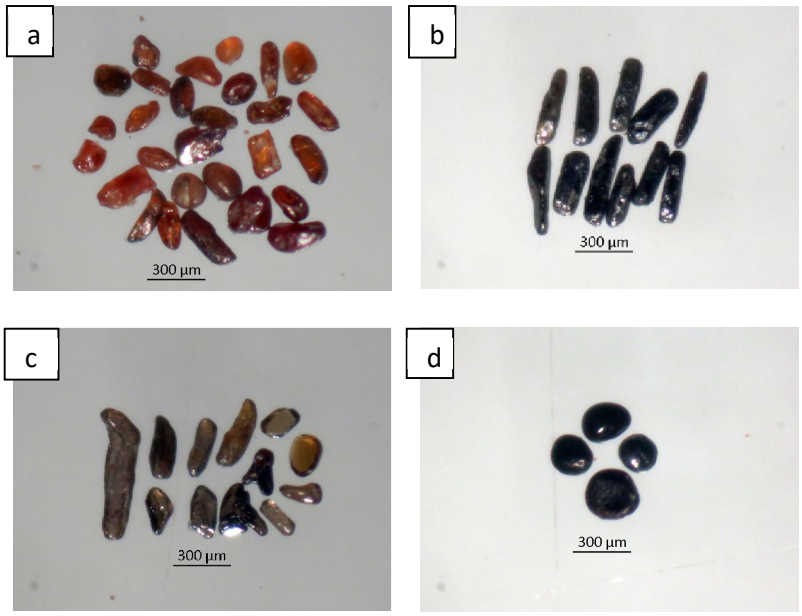


Fig. 19: Photomicrographs of rutile grains shows: a) Red aggregates of different forms, b) Black prismatic grains, c) Honey prismatic, chevron oval grains and d) Oval, semi-rounded and discoidal grains.

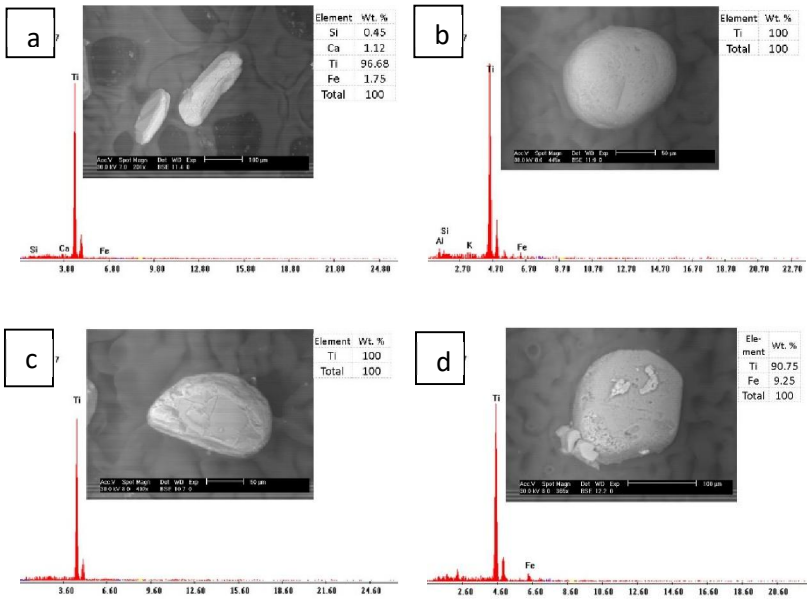


Fig. 20: EDX and BSE image of rutile grains shows: a) Black prismatic grain, b) Red oval grain, c) red irregular grain and d) Black discoidal grain.

Table 10: The average semi quantitative chemical analysis of rutile in the studied area compared with different localities in Egypt.

Element Wt. %	Mauritania (present study)	Barakat (2016) East Rashied	El Azab *et al.* (2019) Damietta	El Alfi (2019) West El-Burullus	Awad *et al.* (2022) El Arish	El Afandy (2022) North delta
Si	--	95.32	0.79	--	7.62	--
Ca	--	--	--	--	--	--
Ti	97.91	--	64.88	97.43	96.16	98.23
Fe	5.50	1.27	5.09	2.89		3.34
Al	--	--	--	--	3.91	--
Sn	--	0.84	--	--	--	--
Cr	--	0.53	--	--	--	--

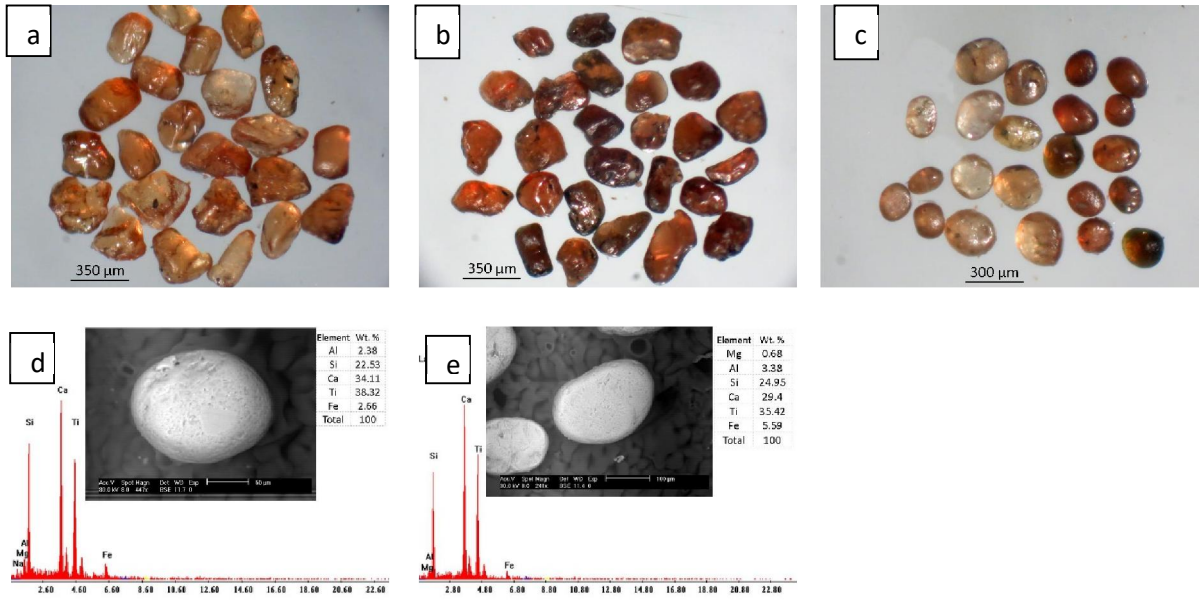


Fig. 21: Photomicrographs of titanite grains shows: a) Honey grains, b) dark honey to black grains, d) colorless to honey on the left side and dark honey to black on the right side, d) EDX and BSE image of semi-rounded grain and e) EDX and BSE image of oval grain.

Table 11: The average semi quantitative chemical analysis of titanite in the studied area compared with different localities in Egypt.

Element Wt. %	Mauritania (present study)	Barakat (2016) East Rashied	El Azab *et al.* (2019) Damietta	El Alfi (2019) West El-Burullus
Mg	0.68	--	--	--
Al	2.88	1.33	1.65	2.14
Si	23.74	28.38	24.68	23.47
Ca	31.76	31.29	26.80	33.08
Ti	36.87	37.22	42.78	39.37
Fe	4.13	1.78	4.09	1.94

Gahnite ($ZnAl_2O_4$)

Gahnite, is a rare mineral belonging to the spinel group. It forms octahedral crystals which may be green and blue (Fig. 22a). Trace spherical grains of gahnite were picked under the stereo binocular-microscope. The gahnite grain subjected to EDX chemical analysis technique. The BSE image is graphically represented along with chemical compositions of the analyzed grain (Fig. 22b).

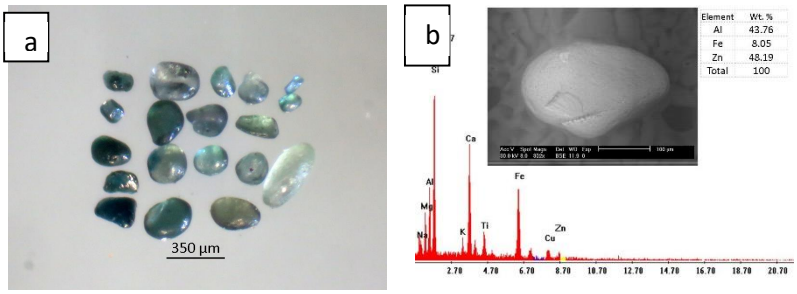


Fig. 22: Photomicrographs of gahnite grains shows: a) Blue and green grains and b) EDX and BSE image of pure grain.

Pyrite

Pyrite is one of the few minerals that are produced by biological micro-environmental systems. It is a common sulphide mineral together with chalcopyrite. It has well developed rounded shape with golden yellow or shiny brassy yellow and occur as isolated colonies (Fig. 23a) or as very small rounded grains attached on the surface of other minerals (Fig. 23b). Pure pyrite grains were investigated under the Environmental Scanning Electronic Microscope (ESEM) are shown in (Fig. 24c) which its EDX shows isolated colonies (Fig. 23c) and very small rounded grains attached on the surface of other minerals (Fig. 23d). Pyrite was separated at magnetic field strength 1.5A using the Frantz Isodynamic separator.

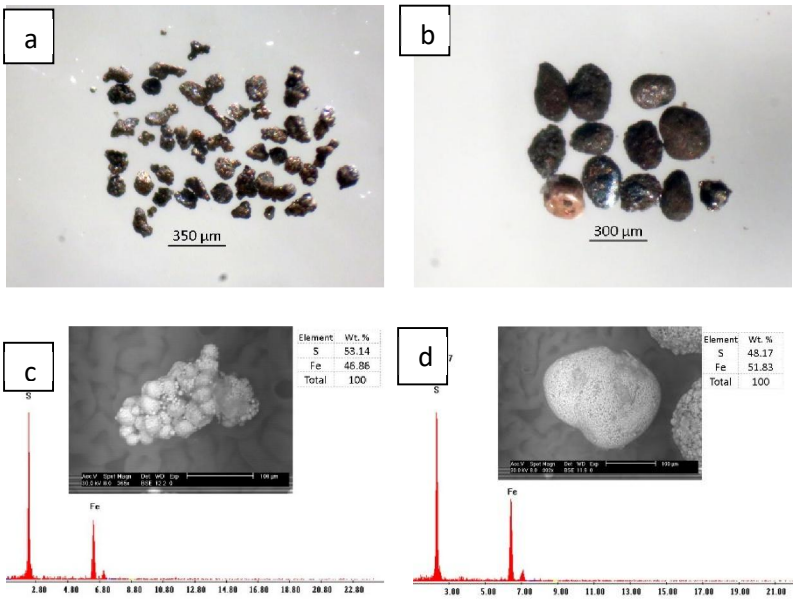


Fig. 23: Photomicrographs of pyrite grains shows: a) Isolated colonies, b) Very small rounded grains attached on the surface of other minerals, c) EDX and BSE image of isolated colonies and d) EDX and BSE image of very small rounded grains attached on the surface of other minerals

4. Conclusion

The sediments in Mauritania distributed in three environments as beach, sand dune, and sabkha. The source of these sediments from some tributaries of El Senegal River. The heavy minerals in these sediments represented by magnetite, ilmenite, garnet, leucoxene, rutile, monazite, and zircon. The comparison between these sediments and the Egyptian sediments in the same environments present these sediments is less than in Egypt as tabulated in table (12).

Table 12: The average of economic heavy minerals comparison between southwest Mauritania and northern Delta Egypt.

	Mauritania (present study)				Dabour *et al.* (1990)		Dabous *et al.* (1992)		E.G.S (1994)	El Azab (2006)			Osman *et al.* (2008)		El Arish (2016)		El Azab *et al.* (2019) Damietta	El Alfi (2019) West El-Burullus	Awad *et al.* (2022) El Arish		El Afandy (2022) North delta
	Beach	Coastal Plain	Sand dune	sabkha	Beach	Sand dune	Beach	Sand dune	Sand dune	Beach	Sand dune	sabkha	Beach	Sand dune	Beach	Sand dune			Beach	Sand dune	
T.H.%	6.777	5.901	5.963	5.161						6.0	5.6	4.0					3.7	4.2	7.0	3.6	4.1
T.Ec. %	2.272	1.675	2.082	1.631	2.88	5.52	2.58	5.154	3.1306	3.1	2.6	1.5	5.194	1.371	5.3	2.49	1.8	1.9	3.5	2.3	2.8
Mg.%	0.335	0.493	0.320	0.268	0.1	0.15	0.54	3.114	0.0338	0.6	0.1	0.27	0.06	0.04	0.1	0.08	0.342	0.529	0.058	0.112	0.585
Ilm. %	1.295	0.915	1.155	0.744	2.09	3.79	0.23		0.2368	0.02	2.0	2.73	3.2	0.97	3	1.8	0.613	1.062	1.341	2.526	1.572
Lux.%	0.398	0.126	0.349	0.337						0.04	0.03	0.02					0.175	0.07	0.073	0.063	
Zr. %	0.083	0.051	0.092	0.093	0.17	0.33	0.63	0.37	1.83	0.04	0.03	0.08	1.08	0.19	0.9	0.2	0.31	0.07	0.20	0.41	0.15
Gar. %	0.112	0.041	0.113	0.122	0.32	1.06	0.15	0.46	0.15	0.03	0.04	0.11	0.75	0.1	0.8	0.3	0.09	0.107	0.167	0.716	0.266
Mz. %	0.014	0.009	0.013	0.02	0.01		0.6	0.11	0.35	0.01	0.01	0.02	0.014	0.001	0.43	0.01	0.01	0.0055	0.007	0.024	0.006
Rut. %	0.035	0.039	0.039	0.047	0.19	0.19	0.43	1.1	0.53	0.09	0.16	0.49	0.09	0.07	0.07	0.1	0.12	0.04	0.06	0.09	0.06
Tit.%																		0.005	0.006	0.005	0.008

T. H., = Total Heavy Minerals, T. Ec. = Total Economic Minerals, Mg.= magnetite, Ilm. = Ilmenite, Lux. = Leucoxene, Zr. = Zircon, Gar. = Garnet, Mz. = Monazite, Rut. = Rutile, Tit= Titanite.

References

Arafa, E. H. M., 1990. Mineralogical and sedimentological studies of some sediments from Egypt and Sudan. Ph.D. Thesis, Fac. Sci., Cairo Univ., Egypt.

Armstrong, P., 1922. Zircon as a criterion of igneous or metamorphic origin. Am. J. Sci., 4(23):391-395.

Awad, M., A. M. El Mezayen, S. M. El Alfi, H. H. Ali and M. Y. Hanfi, 2023. Separation, reserve estimation and radioactivity responsibility of the economic heavy minerals of East El-Arish black sand, North Sinai, Egypt. Sci. Rep., 13:4608.

Barakat, M. G., 2016. Evaluation and mineralogy of beach economic minerals especially ilmenite for the top meter in the Egyptian black sand, east Rosetta, Egypt. Ph.D. Thesis, Fac. Sci., Zagazig Univ., Egypt, 284 p.

Basta, E. Z., 1970. Different types of ilmenite-magnetite intergrowth and their origin. Bull. Fac. Sci., Cairo Univ., 44:195-212.

Boctor, N. Z., 1966. Ore microscopic studies of the opaque minerals in Rosetta-Damietta black sands. M.Sc. Thesis, Fac. Sci., Cairo Univ., Egypt.

Breed, C. S. and T. Grow, 1979. Morphology and distribution of dunes in sand seas observed by remote sensing. In: McKee E. D. (Ed.), A Study of Global Sand Seas. U.S. Geol. Surv. Prof. Pap., 1052:253-302.

Dewedar, A. H. M., 1998. Comparative studies on the heavy minerals in some black sand deposits from Sinai and east Rosetta, with contribution to the mineralogy and economics of their garnet. Ph.D. Thesis, Fac. Sci., Menoufia Univ., Egypt, 197 p.

El Afandy A., M. Khalil, A. El Azab, S. El Alfi, M. Etman and H. R. Saad, 2022. Throw light on the heavy economic minerals of the northern part of Delta, Egypt. Middle East J. Appl. Sci., 12(4):553-581.

El Alfi, S. M., 2019. Inferred resources of heavy economic minerals in West El Burullus area, Egypt. J. Sedimentol. Soc. Egypt, 24:129-147.

El Azab, A., S. M. El Alfi and H. H. Ali, 2019. Economic heavy minerals evaluation of Damietta harbor channel sediments, Egypt. J. Sedimentol. Soc. Egypt, 24:43-61.

El Balakssy, S. S., 2003. Mineralogical studies for the economic minerals in the sand dunes belt at Baltim area, Egypt. Ph.D. Thesis, Fac. Sci., Ain Shams Univ., Egypt, 234 p.

El-Kammar, A. A., A. A. Ragab and M. I. Moustafa, 2010. Geochemistry of economic heavy minerals from Rosetta black sand of Egypt. J. King Abdulaziz Univ. Earth Sci., 21(2):1-25.

Elsner, H., 2010. Heavy minerals of economic importance. Assessment Manual, Federal Institute for Geosciences and Natural Resources (BGR), Hannover, Germany, 218 p.

Flinter, B. H., 1959. The magnetic separation of some alluvial minerals in Malaya. Am. Mineral., 44(7-8):738-751.

Folk, R. L., 1980. Petrology of Sedimentary Rocks. Hemphill Publishing Company, Austin, Texas, USA, 184 p.

Frost, M. T., I. E. Grey, I. R. Harrowfield and C. Li, 1983. Alteration profiles and impurity element distributions in magnetic fractions of weathered ilmenite. Am. Mineral., 68(7-8):817-822.

Groves, A. W., 1930. The heavy mineral suites and correlation of the granites of Northern Brittany, the Channel Islands, and the Cotentin. Geol. Mag., 67(5):218-240.

Hassaan, A. H. A., 2005. Evaluation of the heavy minerals in the coastal sand dunes, East Sabkhat El-Tina, North Sinai, Egypt. Ph.D. Thesis, Fac. Sci., Ain Shams Univ., Egypt.

Hugo, V. E. and D. H. Cornell, 1991. Altered ilmenites in Holocene dunes from Zululand, South Africa: Petrographic evidence for multistage alteration. S. Afr. J. Geol., 94(5-6):365-378.

Keller, E. A., 2000. Environmental Geology. 8th Ed., Prentice Hall, Upper Saddle River, New Jersey, USA, 562 p.

Kinsman, D. J. J., 1969. Modes of formation, sedimentary associations, and diagenetic features of shallow-water and supratidal evaporites. AAPG Bull., 53(4):830-840.

Mansour, S. M. M., 2009. Geology, mineralogy and radioactivity studies on Nuweibi area, Central Eastern Desert, Egypt. M.Sc. Thesis, Fac. Sci., Benha Univ., Egypt.

Mohamed, E. H., 1987. Mineralogical studies for some Quaternary sediments in northern Sinai. M.Sc. Thesis, Fac. Sci., Suez Canal Univ., Ismailia, Egypt.

Mohamed, S. S. M., 1998. Radioactivity and mineralogical studies on Wadi Abu Dabbab alluvial deposits, Central Eastern Desert, Egypt. M.Sc. Thesis, Fac. Sci., Ain Shams Univ., Egypt, 204 p.

Mücke A., 2003. Magnetite, ilmenite and ulvöspinel in rocks and ore deposits: Petrography, microprobe analyses and genetic implications. Mineral. Petrol., 77(3-4):215-234.

Nuclear Materials Authority, (NMA) 2003. Exploration and evaluation of the black sand deposits on the Mediterranean Sea (Volume 2: Geological Studies, Drilling, and Collected Samples). Internal Report, Nuclear Materials Authority (NMA), Cairo, Egypt.

Phillips, W. R. and D. T. Griffen, 1981. Optical Mineralogy: The Nonopaque Minerals. W. H. Freeman and Company, San Francisco, USA, 677 p.

Poldervaart, A., 1955. Zircon in rocks. 1. Sedimentary rocks. Am. J. Sci., 253(8):433-461.

Poldervaart, A., 1956. Zircon in rocks. 2. Igneous rocks. Am. J. Sci., 254(9):521-554.

Rozendaal, A. and C. Philander, 2000. Mineralogy of heavy mineral placers along the west coast of South Africa. In: Rammlmair D., J. Mederer, T. Oberthür, R. B. Heimann and H. Pentinghaus (Eds.), Applied Mineralogy in Research, Economy, Technology, Ecology and Culture. Proc. 6th Int. Congr. Appl. Mineral. (ICAM 2000), Göttingen, Germany, A. A. Balkema, Rotterdam, 417-420.

Saxena, S. K., 1966. Evolution of zircon in sedimentary and metamorphic rocks. Sedimentology, 6(1):1-33.

Summerfield, M. A., 1991. Global Geomorphology: An Introduction to the Study of Landforms. Longman Scientific & Technical / John Wiley & Sons, Inc., New York, USA, 537 p.

Temple, A. K., 1966. Alteration of ilmenite. Econ. Geol., 61(4):695-714.

Van Emden, B., M. R. Thornber, J. Graham and F. J. Lincoln, 1997. The incorporation of actinides in monazite and xenotime from placer deposits in Western Australia. Can. Mineral., 35(1):95-104.

Zhang W., Z. Zhu and C. Y. Cheng, 2011. A literature review of titanium metallurgical processes. Hydrometallurgy, 108(3-4):177-188.